Published in **Computers & Chemical Engineering** (accepted)

http://dx.doi.org/10.1016/j.compchemeng.2007.10.012

Selection of optimal feed flow sequence for a multiple effect evaporator system

R. Bhargava[a], S. Khanam[b,*], B. Mohanty[a] and A. K. Ray[c]

[a] Department of Chemical Engineering, Indian Institute of Technology Roorkee, Roorkee – 247 667, India

[b] Department of Chemical Engineering, National Institute of Technology Rourkela, Rourkela – 769 008, India

[c] Department of Paper Technology, Indian Institute of Technology Roorkee, Roorkee – 247 667, India

* Corresponding author:
E-mail address: shabinahai@gmail.com, skhanam@nitrkl.ac.in
Phone No. +91-9938185505, +91-661-2464251

Abstract

A nonlinear model is developed for a SEFFFE system employed for concentrating weak black liquor in an Indian Kraft Paper Mill. The system incorporates different operating strategies such as condensate-, feed- & product- flashing and steam- & feed- splitting. This model is capable of simulating a MEE system by accounting variations in τ, U, Q_{loss}, physico-thermal properties of the liquor, F and operating strategies.

The developed model is used to analyze six different F including backward as well as mixed flow sequences. For these F, the effects of variations of input parameters, T_0 and F, on output parameters such as SC and SE have been studied to select the optimal F for the complete range of operating parameters. Thus, this model is used as a screening tool for the selection of an optimal F amongst the different F.

An advantage of the present model is that a F is represented using an input Boolean matrix and to change the F this input matrix needs to be changed rather than modifying the complete set of model equations for each F. It is found that for the SEFFFE system, backward feed flow sequence is the best as far as SE is concerned.

Keywords: Screening tool, Optimal feed flow sequence, Flat falling film Evaporator system, Steam economy

1. Introduction

An energy audit shows that MEE House of an Indian Paper industry consumes about 24-30 % of its total energy (Rao and Kumar, 1985) and thus any measure to cut down this taxing energy bill by proper selection of operational strategy will improve the profitability of the plant. Keeping this fact in mind, since last few decades researchers have tried to develop

operating strategies for MEE systems, which would consume minimum amount of live steam and in other words would provide maximum SE to the system. These operating strategies include flow sequences of feed for operation, feed-, product- & condensate- flashing and feed- & steam- splitting. However, one of the easiest ways to increase SE of the system is to operate the MEE system with optimal F. However, screening the optimal F, out of the feasible ones, is time consuming and if done experimentally becomes an arduous task. One reasonable way of doing it is to use simulation.

For the analysis of MEE system many investigators have proposed mathematical models. A few of these were developed by Kern (1950), Itahara and Stiel (1966), Holland (1975), Radovic et al. (1979), Lambert et al. (1987), Mathur (1992), Bremford and Muller-Steinhagen (1994), El-Dessouky et al. (1998, 2000) and Bhargava (2004). These models were not used for the selection of optimal F. However, for this purpose Harpor and Tsao (1972) developed a model for the optimization of a MEE system considering forward- and backward- F. Their work was extended by Nishitani and Kunugita (1979) to propose an algorithm for generating non-inferior F amongst all possible F of a MEE system. The non-inferior F were based on the constraints of viscosity of liquid and the formation of scale and/or foam. They suggested that if an optimal F is required, one should examine the set of non-inferior F.

All these mathematical models are generally based on a set of linear/nonlinear equations and accommodate effects of varying physical properties of vapor/steam and liquor with temperature. These models either use fixed value of U for different effects or variable U based on empirical equations or mathematical models.

It is a fact that set of model equations developed for a given operating strategy does not work when the strategy is changed. In fact, it compels one to restructure and reformulate the whole set of governing equations to address the new operating strategy. For example, if operating

strategy such as flow sequences, liquor splitting and conditions of flashing is changed, the governing equations, which describe this operating strategy must be changed (Mathur, 1992). The above fact further adds difficulty in simulating all the operating strategies through a given model without changing the set of its governing equations. On the other hand Stewart and Beveridge (1977) and Ayangbile et al. (1984) developed generalized cascade algorithm in which the model of an evaporator body is solved repeatedly to address the different operating strategies of a MEE system. With the change in operating strategy the sequence of the solution of the model equation of the effect and the input data to it changes. The solution strategy, employed for solving the model, automatically selects the above sequence based on the input data file where the investigator describes the operating strategy.

The modeling technique proposed by Ayangbile et al. (1984) has been further modified and improved in the present work to account for feed sequencing, feed- & steam- splitting and condensate-, feed- and product- flashing. Besides the above, the improved model also considers variations in τ, U, Q_{loss} from surfaces of different effects and physico-thermal properties of steam/vapor, condensate and liquor, which were not accounted in the work of Ayangbile et al. (1987). This model is used as a screening tool for the selection of optimal F for a MEE system.

2. Problem statement

The MEE system selected for above investigation is a SEFFFE system that is being operated in a nearby Indian Kraft Paper Mill for concentrating weak black liquor. The schematic diagram of a SEFFFE system with backward F is shown in Fig. 1. The first two effects of it are considered as finishing effects, which require live steam and the seventh effect is attached to a vacuum unit. This system employs feed- & steam- splitting, feed- and product-flashing along with primary and secondary condensate flashing to generate auxiliary vapor, which are then used in vapor bodies of appropriate effects to improve overall SE of the system.

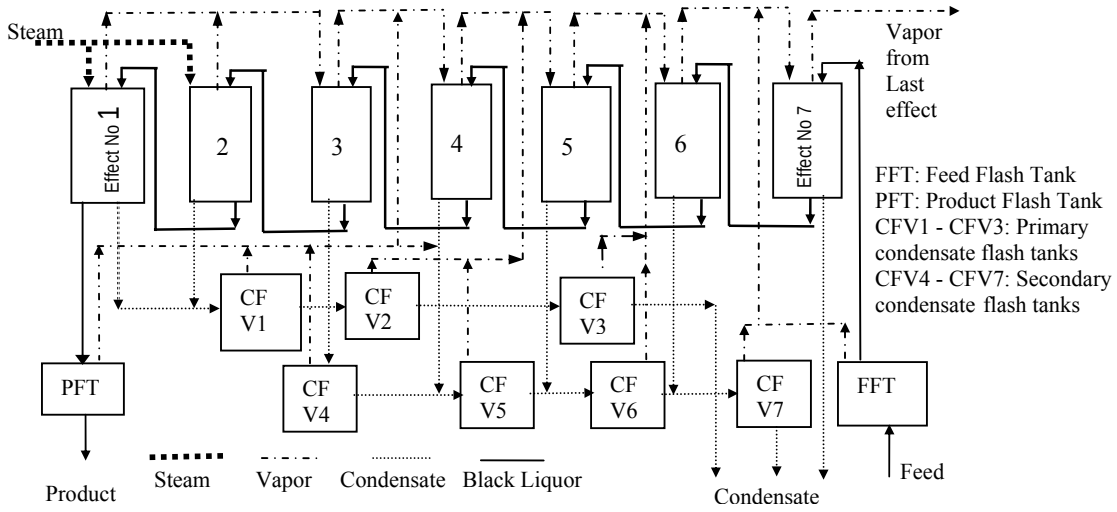

Fig. 1. Schematic diagram of SEFFFE system

2.1. Operating parameters and their variations

Typical operating parameters of a SEFFFE system are given in Table 1 and these are considered as a base case. Further, the results of base case values are used for comparison with other suggested cases of operation involving different F. It is seen from Table 1 that steam temperature going into effect no. 1 is 7 °C cooler that the steam into effect no. 2. This is an actual scenario and thus it has been taken as it is during simulation. The plausible explanation is the unequal distribution of steam from the header to these effects leading to two different pressures in the steam side of these effects. The data presented in Table 2 shows the variation in operating parameters of Indian paper mill. The above information is used to study the effect of variation of operating parameters on SE. The geometrical parameters for this system are shown in Table 3. While studying the different F, geometrical parameters are considered to be constant.

Table 1

Base case operating parameters for the SEFFFE system

S. No	Parameter(s)		Value(s)
1	Total number of effects		7
2	Number of effects being supplied live steam		2
3	Live steam temperature	Effect 1	140 °C
		Effect 2	147 °C
4	Black liquor inlet concentration		0.118
6	Liquor inlet temperature		64.7^{o}C
7	Black liquor feed flow rate		56200 kg/h
8	Last effect vapor temperature		52 °C
9	Feed flow sequence		Backward
10	Feed flash tank position		As indicated in the Fig. 1
11	Product flash tank position		
12	Primary- and secondary- condensate flash tank position		

Table 2

Ranges of operating parameters of a SEFFFE system

S. No.	Parameters		Variation in value
1.	Steam temperature	Effect 1	120^{o}C – 160^{o}C
		Effect 2	127 ^{o}C – 167^{o}C
2.	Liquor flow rate		56200 - 78680 kg/h

Table 3

Geometrical Parameters of the flat falling film evaporators

S.No.	Parameter	Value
1.	Area of effect nos. 1 to 7	540, 540, 660, 660, 660, 660, 690 m^2
2.	Size of lamella	1.5 m (W) x 1.0 m (L)
3.	Type of lamella	Pas-Axero Dimpled Plate Type
4.	Material of construction	SS 2333

2.2. Feasible F

F represents the movement of feed in a MEE system. Generally, F are of three types – forward, backward and mixed. For a forward F feed first enters into first effect where evaporation takes place. Then concentrated feed exits first effect and enters into second effect. This sequence follows up to the last effect. In a MEE system effects are numbered according to the flow of vapor/steam through the system and this numbering methodology is used for specifying a flow sequence.

The SEFFFE system generally uses backward- and mixed- F due to variation in typical physico-thermal properties of black liquor with the change in temperature and concentration of liquor during evaporation. In the present investigation various feasible F, shown in Table 4, are studied in order to obtain the optimal F, which yields highest possible SE. In all these F steam is splitted equally and fed in first two effects. These F are selected based on the flow sequences of MEE systems reported in the literature (Ray et al., 2000) as well as that have been employed in industry. However, the present model can be used to simulate any flow sequence.

Table 4

Feasible F in SEFFFE system

Seq. No.	F	Remarks
a	7→6→5→4→3→2→1	Backward F, feed to 7th effect
b	7↘ 6↗ 5→4→3→2→1	Backward F, feed splits equally among 6th and 7th effects
c	6→7→5→4→3→2→1	Mixed F, feed to 6th effects
d	5→6→7→4→3→2→1	Mixed F, feed to 5th effect
e	4→5→6→7→3→2→1	Mixed F, feed to 4th effect
f	3→4→5→6→7→2→1	Mixed F, feed to 3rd effect

3. Mathematical model

The complete model for the SEFFFE system is developed in following sections:

3.1. Model for an effect

By taking mass and energy balances over i^{th} effect of a SEFFFE system, shown in Fig. 2, following equations can be developed.

Overall mass balance around evaporation section

$$L_{i+1} = L_i + V_i \quad (1)$$

Overall mass balance around steam chest

$$V_{i-1} = CO_{i-1} \quad (2)$$

Component mass balance

$$L_{i+1}\, x_{i+1} = L_i\, x_i = L_F\, x_F \quad (3)$$

Overall energy balance

$$L_{i+1}\, h_{Li+1} = L_i\, h_{Li} + V_i\, H_{Vi} + \Delta H_i \quad (4)$$

Where ; $\Delta H_i = U_i A_i (T_{i-1} - T_{Li})$ (5)

Energy balance on steam/vapor side

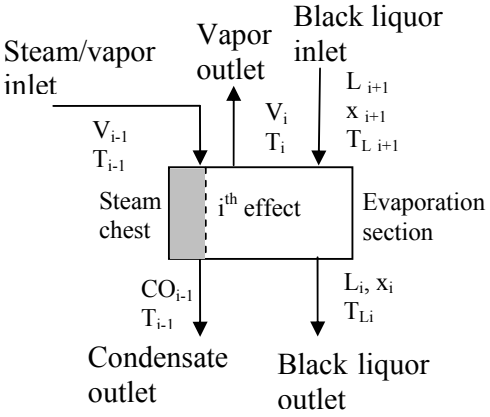

Fig. 2 Block diagram of an evaporator

$$V_{i-1} = \Delta H_i / (H_{Vi-1} - h_{Li-1}) \quad (6)$$

The correlations for enthalpy (h_L) for black liquor is given as:

$$h_L = C_{PP} * (T_L - C_5) \quad J/kg \quad (7)$$

where, $C_{PP} = C_1 * (1-C_4x)$ and $T_L = T + \tau$

The values of coefficients C_1, C_4 and C_5, used in Eq. 7, are 4187, 0.54 and 273, respectively. For the development of a correlation for τ of black liquor, the functional relationship is taken from well established TAPPI correlation (Ray et al., 1992). For i^{th} effect where concentration of black liquor is x_i, τ is given as:

$$\tau_i = C_3 (C_2 + x_i)^2 \quad (8)$$

The correlation of τ is obtained by fitting Eq. 8 against the data of a nearby paper mill as given in Table 5. The value of C_3 is computed as 20, using value of C_2 as 0.1 (Ray et al., 1992). This correlation gives a maximum error of 6% with an average error of 3.4%.

Table 5

Data for the determination of τ

x_i	0.0767	0.091	0.106	0.13	0.169	0.244	0.369	0.462	0.47
τ_i, K	0.60	0.70	0.80	1.10	1.40	2.30	4.30	6.20	6.40

Combining Eqs. 1 to 8 and eliminating V_i, x_i, h_i, ΔH_i and T_{Li} one gets following cubic polynomial in terms of L_i:

$$a_1 L_i^3 + a_2 L_i^2 + a_3 L_i + a_4 = 0 \quad (9)$$

where coefficients a_1, a_2, a_3 and a_4 are functions of input liquor parameters and other known parameters like heat transfer area (A_i) and overall heat transfer coefficient (U_i) of the effect for which it is being used.

The expression for coefficients a_1, a_2, a_3 and a_4 are:

$$a_1 = H_{Vi} - C_1 T_i - C_1 C_2^2 C_3 + C_1 C_5 \quad (9a)$$

$$a_2 = L_{i+1}\, h_{Li+1} + U_i A_i\, (T_{i-1} - T_i - C_3 C_2^2) + L_{i+1}\, x_{i+1}\, (C_1 C_4 T_i - 2C_1 C_2 C_3 + C_1 C_3 C_2^2 C_4 - C_1 C_4 C_5 - L_{i+1}\, H_{Vi}) \quad (9b)$$

$$a_3 = (L_{i+1}\, x_{i+1})^2\, (2C_1 C_2\, C_3 C_4 - C_1 C_3\,) - 2C_2 C_3\, U_i\, A_i\, L_{i+1}\, x_{i+1} \quad (9c)$$

and $$a_4 = (C_1 C_3 C_4\, L_{i+1}\, x_{i+1} - C_3\, U_i\, A_i)\, (L_{i+1}\, x_{i+1})^2 \quad (9d)$$

3.2. Model for liquor flash tank

For a liquor flash tank, shown in Fig. 3, a similar cubic model as developed for an effect, presented in Eq. 9, is proposed to calculate L_e for a known value of L_1. The modified expressions for constants a_1 to a_4 in Eq. 9 are described below:

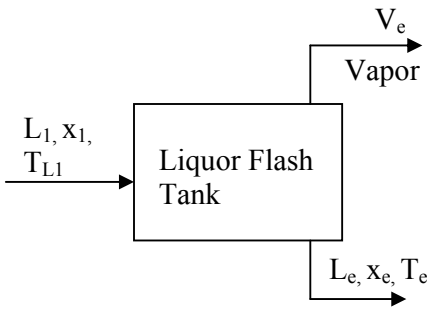

Fig. 3. Block diagram of a liquor flash tank

$$a_1 = H_{Ve} - C_1 T_e - C_1 C_2^2 C_3 + C_1 C_5 \quad (10a)$$

$$a_2 = L_1\, h_{L1} + L_1\, x_1\, (C_1 C_4 T_e - 2C_1 C_2 C_3 + C_1 C_2^2 C_3 C_4 - C_1 C_4 C_5) - L_1\, H_{Ve} \quad (10b)$$

$$a_3 = (L_1 x_1)^2\, (2C_1 C_2\, C_3\, C_4 - C_1 C_3\,) \quad (10c)$$

$$a_4 = (L_1 x_1)^3 C_1 C_3 C_4 \quad (10d)$$

It should be noted here that in the present investigation only one cubic equation with different expressions of coefficients is used to model an effect as well as liquor flash tank (feed and product flash tanks). Hence, in this case only one cubic equation solver is used to predict the exit liquor flow rate from an effect and liquor flash tank which reduces the length of computer program as well as burden of computation.

The cubic equation, Eq. 9, is solved to get its real root(s). Out of the real roots only one root, which has a value equal or less than F, is selected for further processing. Once this root is

known, other parameters like exit liquor -concentration, -temperature, vapor produced (V_i) and the quantity of vapor required (V_{i-1}) are computed using Eqs. 3, 4, 1 & 6, respectively.

3.3. Model for condensate flash tank

Material and energy balances over condensate flash tank yields following relation to determine exit condensate flow rate (CO_j), for a known condensate mass flow rate, CO_i, entering at a temperature, T_i, with specific enthalpy, h_i, and being flashed at temperature, T_j to generate vapor of amount, V_j. The overall mass and energy balance give:

$$CO_j = CO_i (H_{vj} - h_i)/ (H_{vj} - h_j) \quad (11)$$

and $$V_j = CO_i - CO_j \quad (12)$$

3.4. Empirical correlations for U and Q_{loss}

The present model for a SEFFFE system uses empirical correlations for the prediction of U and Q_{loss} from each effect. For development of these empirical correlations the data is collected from a Indian Kraft Paper Mill employing SEFFFE system.

A simplified empirical model for Q_{loss} from different effects, piping, heat exchangers, flash tanks, etc. of a SEFFFE system is developed based on the correlation of heat transfer for natural convection ($Nu=C(Gr.Pr)^n$) (Coulson and Richardson, 1996) and plant data. The power law equation, which is a modified form of heat transfer due to natural convection, is proposed to calculate Q_{loss} as:

$$Q_{loss} = 1.9669\times10^3 (\Delta t)^{1.25} \quad (13)$$

Where Δt is the temperature difference exists between temperature of effect and that of atmosphere. Predictions from the Eq. 13 show an error limit of –33 to +29 %. In the present SEFFFE system the average Q_{loss} is of the tune of 5.8 % of total energy input to the system through steam and liquor. It appears that the present Q_{loss} is at a higher side in the plant may be due to degraded insulation.

To develop the empirical correlation for U of an effect, parameters ΔT across the steam chest of an effect, x_{avg} and F_{avg} have been considered as these parameters show a high level of cross correlation amongst themselves. The statistical analysis of cross correlation between these parameters is shown in Table 6.

Table 6
Cross correlation coefficients between the parameters U, delta T (ΔT), X_{avg} and F_{avg}.

	OHTC	*delta T*	*Xavg*	*Favg*
OHTC	1			
delta T	-0.96999	1		
Xavg	0.928086	-0.92326	1	
Favg	-0.81645	0.875356	-0.90815	1

Further, a plot of calculated values of U of all seven effects for four different sets of plant data is shown in Fig. 4. The analysis of this figure clearly shows that the trend of U for first two effects i.e. effect No. 1 and 2 is totally different than the trend of effect Nos. 3 to 7. The values of U are substantially low for effect No.1 & 2 which is primarily due to the higher concentration of black liquor in first two effects (43% to 53%). In fact, in the vicinity of 48% solid concentration the scale formation starts (Süren, 1995). This phenomenon causes U to fall drastically in effect No. 1 & 2.

Therefore, two different empirical correlations are developed, one for effect Nos. 1 to 2 and the other for effect Nos. 3 to 7. The normalized Power law equation, shown in Eq. 14, is used for both the correlations using divisors 2000 $W/m^2/K$, 40 °C, 0.6 and 25 kg/s as these are higher than the respective highest values encountered in the plant data.

$$(U/2000) = a\,(\Delta T/40)^b\,(x_{avg}/0.6)^c\,(F_{avg}/25)^d \qquad (14)$$

The computed values of U from plant data, for all the seven effects, are used to estimate the unknown coefficients a, b, c and d of Eq. 14 using constrained minimization technique of

Sigma Plot-a scientific data analysis and plotting software. The estimated coefficients for both the correlations (Eqs. 14(a) and (b)) are given in Table 7.

Table 7

Value of Coefficients of Eq. 14

Effect No.	a	b	c	d	% Error Band	Eq. No.
1 and 2	0.0604	-0.3717	-1.227	0.0748	-11.32 to 7.25	(14a)
3 to 7	0.1396	-0.7949	0.0	0.1673	-11.75 to 8.20	(14b)

Fig. 5 has been plotted to show the extent of fitting of the U. From this figure it is clear that the correlations, Eq. 14a and 14b, predict the U data within an error limit of $\pm$10%.

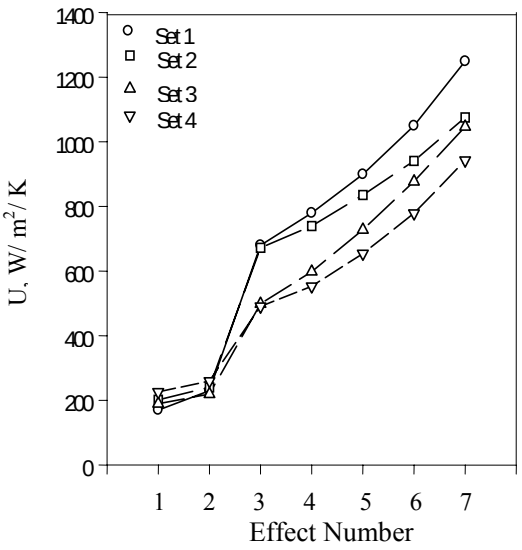

Fig. 4. Profiles of U from Plant Data

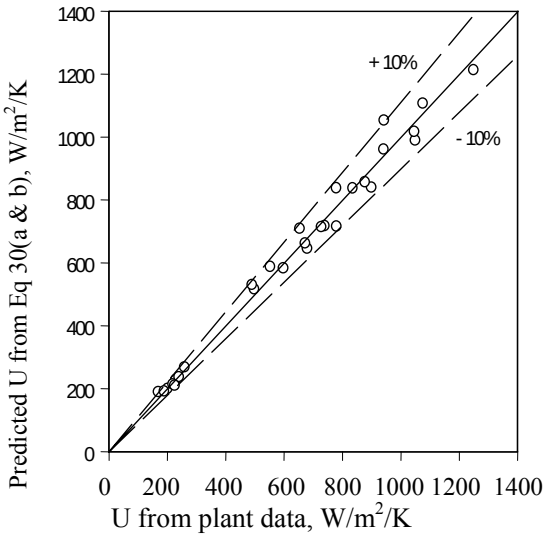

Fig. 5. Comparison of U from plant data for all effects and those predicted from Eq. 14 (a & b)

3.5. Development of generalized model for a MEE system

A MEE system consisting of 'n' effects has been modeled by Ayangbile et al. (1987). This model is improved to develop a generalized model which can account different flow sequencing, feed & steam splitting and condensate-, feed- and product- flashing.

The modified block diagram of i^{th} effect is shown in Fig. 6, which accommodates any flow sequencing and liquor splitting. The black liquor feed rate to i^{th} effect can be expressed as:

$$y_{oi}\, L_F + \sum_{\substack{j=1 \\ j\neq i}}^{n} y_{ji} L_j \tag{15}$$

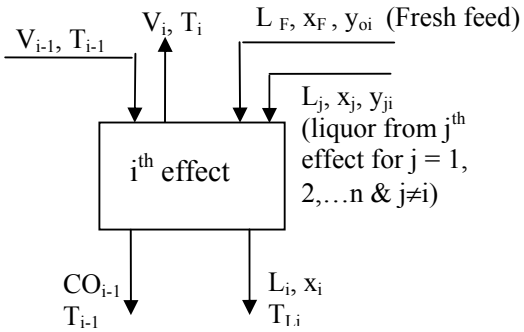

Fig. 6. Block Diagram of an evaporator for cascade simulation

Where y_{oi} is the fraction of the feed (after feed flash), which enters into i^{th} effect and y_{ji} is the fraction of black liquor which is coming out from j^{th} effect and enters into the i^{th} effect.

Total mass balance around i^{th} effect gives;

$$y_{o,i}\, L_F + \sum_{j=1}^{n} y_{j,i} L_j = L_i + V_i$$

or
$$\sum_{j=1}^{n} y_{j,i} L_j - L_i = V_i - y_{o,i} L_F \tag{16}$$

This equation, developed for i^{th} effect and shown in Eq. 16, can be represented for all n effects by a Matrix Equation as given below:

$$\begin{bmatrix} y_{11}-1 & y_{21} & y_{31} & \cdots & y_{n1} \\ y_{12} & y_{22}-1 & y_{32} & \cdots & y_{n2} \\ y_{13} & y_{23} & y_{33}-1 & \cdots & y_{n3} \\ \vdots & \vdots & \vdots & \cdots & \vdots \\ y_{1n} & y_{2n} & y_{3n} & \cdots & y_{nn}-1 \end{bmatrix} \begin{bmatrix} L_1 \\ L_2 \\ L_3 \\ \vdots \\ L_n \end{bmatrix} = \begin{bmatrix} V_1 - y_{o1} L_F \\ V_2 - y_{o2} L_F \\ V_3 - y_{o3} L_F \\ \vdots \\ V_n - y_{on} L_F \end{bmatrix}$$

i.e. $$\mathbf{[Y\text{-}I]\, L = V} \tag{17}$$

or, $$\mathbf{L = [Y\text{-}I]^{-1}\, V = AV} \tag{18}$$

Where, **A** is the inverse of the matrix **[Y-I]**. As the value of y_{jj} is equal to zero, the diagonal elements of matrix **[Y-I]** become -1.

From Eq. 18, the exit liquor flow rate, L_i, from i^{th} effect as shown in Fig. 6, can be written as:

$$L_i = \sum_{j=1}^{n} a_{ij} V_j - L_F \sum_{j=1}^{n} y_{oj} a_{ij} \tag{19}$$

Similarly, component mass balance around i^{th} effect provides:

$$y_{oi} L_F x_F + \sum_{j=1}^{n} y_{ji} L_j x_j = L_i x_i$$

or, $$\sum_{j=1}^{n} y_{ji} L_j x_j - L_i x_i = -y_{oi} L_F x_F$$

or, $$\mathbf{[Y\text{-}I]\ LX} = \mathbf{-\ Y_0}\, L_F\, x_F$$

Where, $\mathbf{LX} = [\, L_1 x_1 \quad L_2 x_2 \quad L_3 x_3 \quad \ldots \quad L_n x_n \,]$

or, $$\mathbf{LX} = \mathbf{[Y\text{-}I]}^{-1} (\mathbf{-\ Y_0}\, L_F x_F) = \mathbf{A}(\mathbf{-\ Y_0}\, L_F x_F) \tag{20}$$

Using Eq. 20, the total solids coming out of i^{th} effect is:

$$L_i x_i = -\left(\sum_{j=1}^{n} y_{oj} a_{ij} \right) L_F x_F \tag{21}$$

Combining Eq. 19 and 21

$$x_i = \frac{\left(\sum_{j=1}^{n} y_{oj} a_{ij} \right) L_F x_F}{\left(\sum_{j=1}^{n} y_{oj} a_{ij} \right) L_F - \sum_{j=1}^{n} a_{ij} V_j} \tag{22}$$

For the development of a general model of an evaporator system, mathematical model for i^{th} effect as given by Eq. 9, 9a to 9d is generalized by replacing the inlet liquor flow term, L_{i+1}, by expression given in Eq. 15.

The model for an evaporator, shown in Fig. 6, is solved to obtain L_i, x_i, V_i and V_{i-1}. The vapor required in i^{th} effect steam chest, V_{i-1}, is re-designated as V_{bi}. Whereas, the actual pool of vapor available for i^{th} effect steam chest consists of several vapor streams at same operating

pressure, namely vapor produced in $(i-1)^{th}$ effect and the vapor produced by feed-, product- and condensate- flashing and is designated as V_{i-1}. This has been clearly shown in Fig. 7. The amount of vapor denoted by V_{i-1} and V_{bi} should be equal for an exact solution. An index called "Performance Index (PI)" is defined as a measure of the difference in the values of V_{i-1} and V_{bi}.

$$PI = \Sigma ((V_{i-1} - V_{bi}) / V_{bi})^2 \quad (23)$$

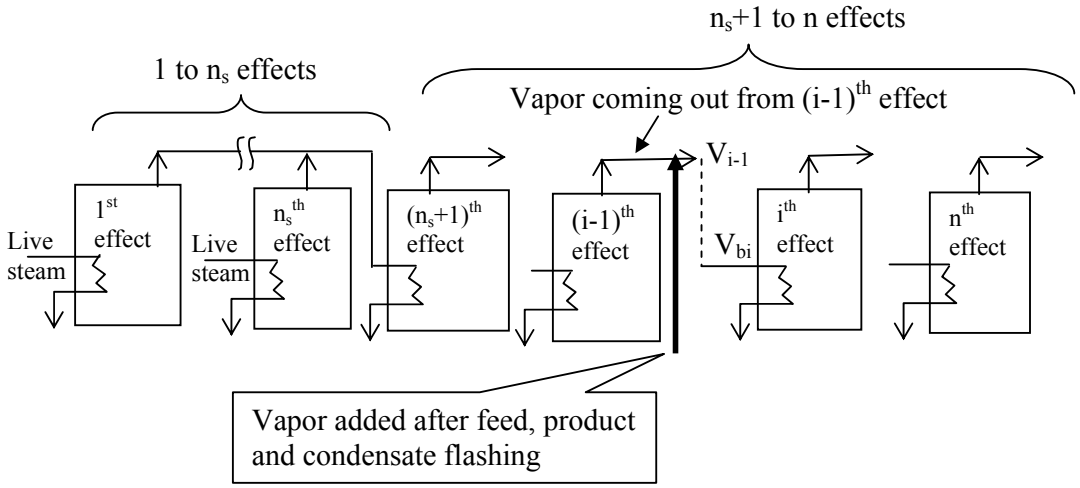

Fig. 7 The schematic diagram of vapor flow in a MEE system consists of 'n' effects

The summation term shown in Eq. 23 is for 'n_s+1' to 'n' effects, where n_s effects are fed with live steam and in present case is equal to two. The summation of V_{bi} for first n_s effects gives total SC, and summation of V_i from first n_s effects is the vapor to $(n_s + 1)^{th}$ effect, as shown in Fig. 7.

The operating parameters T_i, T_{Li}, V_i and x_i of i^{th} effect are functions of vapor body pressure, P_i. If variations of parameters are within a small range then one can always approximate it to be a linear one.

As proposed by Ayangbile et al. (1984), it is assumed that vapor produced in an effect, V_i, is a function of temperature difference (driving force, ΔT_i) responsible for heat transfer.

Where, $\Delta T_i = T_{i-1} - T_{Li}$ (24)

hence, $$\delta V_i = \frac{\partial V_i}{\partial(\Delta T_i)}(\delta \Delta T_i)$$

defining $$\frac{\partial V_i}{\partial(\Delta T_i)} = \alpha_i$$

$$\delta V_i = \alpha_i \, \delta(\Delta T_i) \quad = \alpha_i(\delta T_{i-1} - \delta T_{Li}) \tag{25}$$

To determine change in pressure, P_i, with a perturbation in saturation temperature, T_i, one can get:

$$\delta T_i = \frac{\partial T_i}{\partial P_i}\delta P_i = \gamma_i \; \delta P_i \tag{26}$$

where, $\gamma_i = \dfrac{\partial T_i}{\partial P_i}$

The black liquor temperature is functions of pressure and solid concentration and hence,

$$\delta T_{Li} = \frac{\partial T_{Li}}{\partial P_i}\delta P_i + \frac{\partial T_{Li}}{\partial x_i}\delta x_i = \gamma_i' \; \delta P_i \; + \gamma_i'' \; \delta x_i \tag{27}$$

From Eq. 22, one can write:

$$\delta x_i = \frac{\sum_{j=1}^{n} (y_{oj} a_{ij}) L_F x_F \sum_{j=1}^{n} a_{ij} \delta V_j}{\left[\sum_{j=1}^{n} (y_{oj} a_{ij}) L_F - \sum_{j=1}^{n} a_{ij} V_j\right]^2} \tag{28}$$

Combining Eq. 27 and 28, the following expression can be obtained:

$$\delta T_{Li} = \gamma_i' \, \delta P_i + \theta_i \sum_{j=1}^{n} a_{ij} \delta \, V_j \tag{29}$$

where, $$\theta_i = \frac{\gamma_i'' \times \sum_{j=1}^{n} (y_{oj} a_{ij}) L_F x_F}{\left[\sum_{j=1}^{n} (y_{oj} a_{ij}) L_F - \sum_{j=1}^{n} a_{ij} V_j\right]^2}$$

Defining $\Delta V_i = V_{i-1} - V_{bi}$ for $i = n, n-1, \ldots, n_s+1$ (30)

and for k^{th} iteration, changes in V_{i-1} and V_{bi} are defined as:

$$\delta V_{i-1} = V_{i-1}^{k} - V_{i-1}^{k-1} \tag{31a}$$

and $$\delta V_{bi} = V_{bi}^{k} - V_{bi}^{k-1} \tag{31b}$$

For the solution of MEE system, the vapor available from $(i-1)^{th}$ effect should be equal to vapor required in i^{th} effect, that is,

$$V_{i-1}^{k} \approx V_{bi}^{k} \tag{32}$$

On combining Eqs. 30, 31 and 32 and rearranging, following equation is formed:

$$\Delta V_i = \delta V_{bi} - \delta V_{i-1} \tag{33}$$

As vapor required for heating in an effect is a function of vapor produced in that effect, on linearization, one gets;

$$\delta V_{bi} = \frac{\partial V_{bi}}{\partial V_i} \delta V_i = \beta_i \, \delta V_i \tag{34}$$

Combining Eq. 25, 26, 29, 33 and 34, one gets

$$\delta V_i - \beta_{i+1} \, \delta V_{i+1} = -\Delta V_{i+1} \qquad \text{where, } i = 1,2,\ldots,(n - n_s) \tag{35}$$

and $$(1 + \alpha_i \theta_i a_{ii}) \delta V_i + \alpha_i \theta_i \sum_{j=1}^{i-1} a_{ij} \, \delta V_j + \alpha_i \theta_i \sum_{j=i+1}^{n} a_{ij} \, \delta V_j - \alpha_i \gamma_i \, \delta P_{i-1} + \alpha_i \gamma_i' \, \delta P_i = 0 \tag{36}$$

where, $i = 1,2,\ldots,(n-n_s+1)$

Eqs. 35 and 36 form a set of $(2(n-n_s)+1)$ linear algebraic equations with same number of unknowns, namely, δV_i, where, $i = 1,2,\ldots, n-n_s+1$ and δP_i where, $i= 1,2,\ldots, n-n_s$.

Matrix representation of $[2(n-n_s)+1]$ linear algebraic set of equations given by Eqs. 35 and 36 is given in following equation form:

D Z = E

Where the size of the coefficient matrix **D** is $[2(n-n_s)+1] \times [2(n-n_s)+1]$. Similarly, the size of **Z** and **E** matrices is $1 \times [2(n-n_s)+1]$ each. These matrices are detailed in Table 8 for the SEFFFE system.

Table 8

Matrix representation of set of linear algebraic equations

1	$-\beta_2$	0	0	0	0	0	0	0	0	0	δV_1		$-\Delta V_2$
0	1	$-\beta_3$	0	0	0	0	0	0	0	0	δV_2		$-\Delta V_3$
0	0	1	$-\beta_4$	0	0	0	0	0	0	0	δV_3		$-\Delta V_4$
0	0	0	1	$-\beta_5$	0	0	0	0	0	0	δV_4		$-\Delta V_5$
0	0	0	0	1	$-\beta_6$	0	0	0	0	0	δV_5		$-\Delta V_6$
$1+b_{11}$	b_{12}	b_{13}	b_{14}	b_{15}	b_{16}	$\alpha_1\gamma'_1$	0	0	0	0	δV_6	=	0
b_{21}	$1+b_{22}$	b_{23}	b_{24}	b_{25}	b_{26}	$-\alpha_2\gamma_2$	$\alpha_2\gamma'_2$	0	0	0	δP_1		0
b_{31}	b_{32}	$1+b_{33}$	b_{34}	b_{35}	b_{36}	0	$-\alpha_3\gamma_3$	$\alpha_3\gamma'_3$	0	0	δP_2		0
b_{41}	b_{42}	b_{43}	$1+b_{44}$	b_{45}	b_{46}	0	0	$-\alpha_4\gamma_4$	$\alpha_4\gamma'_4$	0	δP_3		0
b_{51}	b_{52}	b_{53}	b_{54}	$1+b_{55}$	b_{56}	0	0	0	$-\alpha_5\gamma_5$	$\alpha_5\gamma'_5$	δP_4		0
b_{61}	b_{62}	b_{63}	b_{64}	b_{65}	$1+b_{66}$	0	0	0	0	$-\alpha_6\gamma_6$	δP_5		0

Where $b_{ij} = \alpha_i a_{ij} \theta_i$

α_i, β_i, γ_i and γ_i' for different iteration number, denoted by k, are defined as

$$\alpha_i = V_i^k / \Delta T_i^k \qquad k=1$$

$$= (V_i^k - V_i^{k-1}) / (\Delta T_i^k - \Delta T_i^{k-1}) \qquad k = 2,3,\ldots \qquad (37)$$

$$\beta_i = V_{bi}^k / V_i^k \qquad k=1$$

$$= (V_{bi}^k - V_{bi}^{k-1}) / (V_i^k - V_i^{k-1}) \qquad k=2,3\ldots \qquad (38)$$

$$\gamma'_i = \frac{\partial T_{Li}}{\partial P_i} = \frac{\partial (T_i + BPR_i)}{\partial P_i} = \frac{\partial T_i}{\partial P_i} \qquad (39)$$

$$\gamma_i = \frac{\partial T_{i-1}}{\partial P_{i-1}} \qquad (40)$$

$$\gamma''_i = \frac{\partial T_{Li}}{\partial x_i} = \frac{\partial (T_i + BPR_i)}{\partial x_i} = 2 * C_3 (C_2 + x_i) \qquad (41)$$

Where, derivatives, γ_i' and γ_i, given by Eqs. 39 and 40, respectively.

By solving Eqs. 35 and 36, one can obtain the values of δP_i, where, i = 1,2,…,$(n-n_s)$. The values of δP_i, so obtained, are used to modify the pressure of all the effects except last effect- the pressure of which is kept at a fixed value.

This process is to be repeated iteratively till desired precision ($5*10^{-6}$) in the value of PI is obtained.

4. Solution of the model

For the solution of the model, developed in the present investigation, a computer program is developed in FORTRAN 90 and run on Pentium IV machine, using Microsoft FORTRAN Power Station 4.0 compiler. The flow chart of the algorithm is shown in Fig. 8.

For the generalized cascade algorithm the equation developed for an effect is solved repeatedly for different effects depending upon the sequence of computation determined by the selected F which in turn is decided by the Boolean matrix ***B***.

For the SEFFFE system, order of the matrix is 8×8, where the first column denotes the feed stream and subsequent columns are source effects 1 to 7 and first 7 rows are sink effects and last row is product stream. A unit value of element b_{ij} indicates that liquor exiting from $(j-1)^{th}$ effect enters i^{th} effect. The backward F is represented by the Boolean matrix, given below, in which element $b_{13} = 1$ shows that liquor exits from 2^{nd} effect and enters first effect.

(Feed) F 1 2 3 4 5 6 7

Source effect ←

↓ Sink effect

$$\boldsymbol{B} = \begin{bmatrix} 0 & 0 & 1 & 0 & 0 & 0 & 0 & 0 \\ 0 & 0 & 0 & 1 & 0 & 0 & 0 & 0 \\ 0 & 0 & 0 & 0 & 1 & 0 & 0 & 0 \\ 0 & 0 & 0 & 0 & 0 & 1 & 0 & 0 \\ 0 & 0 & 0 & 0 & 0 & 0 & 1 & 0 \\ 0 & 0 & 0 & 0 & 0 & 0 & 0 & 1 \\ 1 & 0 & 0 & 0 & 0 & 0 & 0 & 0 \\ 0 & 1 & 0 & 0 & 0 & 0 & 0 & 0 \end{bmatrix}$$

1
2
3
4
5
6
7
P (Product)

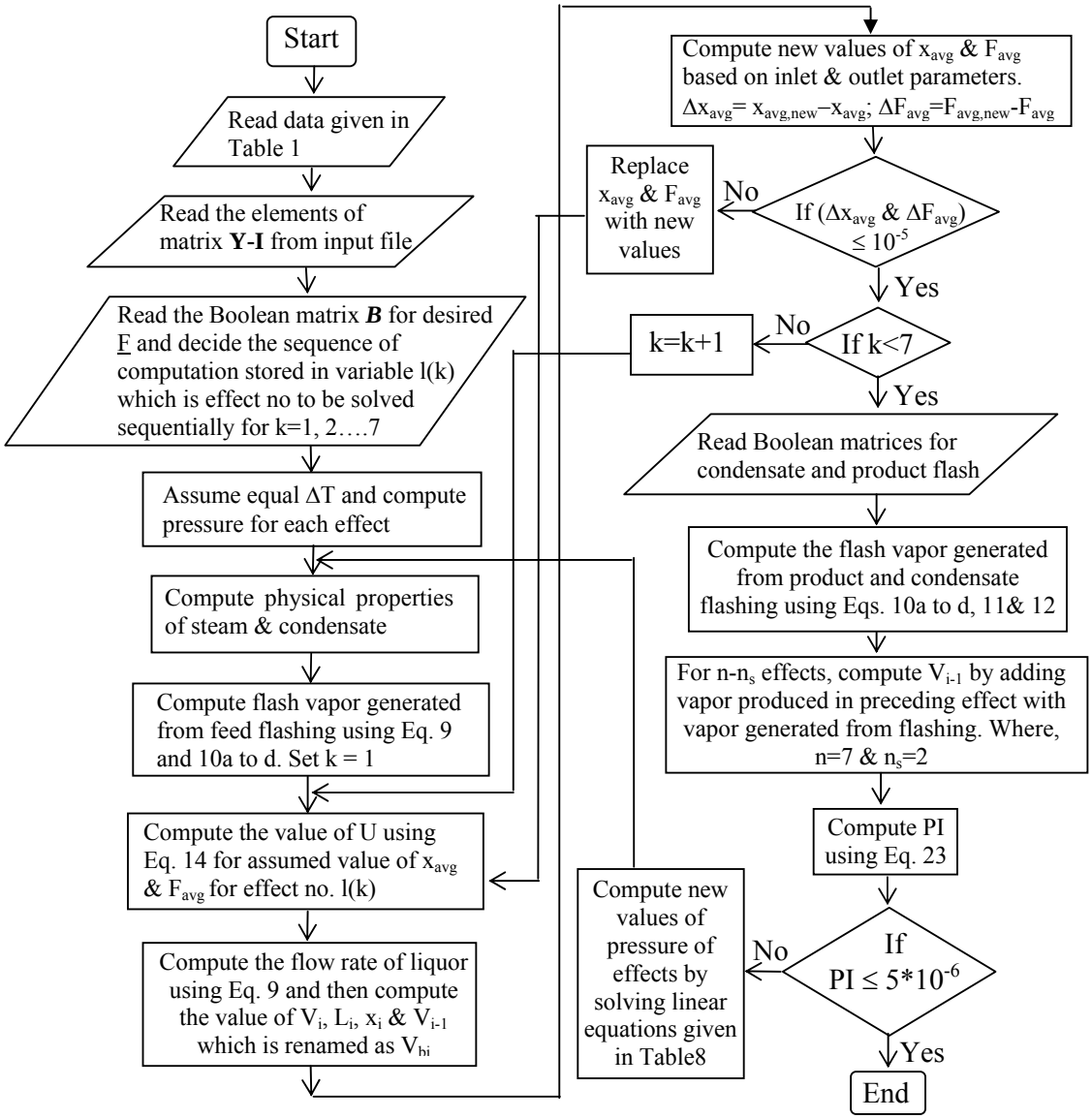

Fig. 8. Flow chart for solution of the model

If a liquor stream exiting from $(j-1)^{th}$ effect is splitted for supply to more than one effect then it will be depicted by more than one entry of unit value in the j^{th} column. Similarly, if a sink effect (i^{th}) receives liquor from more than one source effect then, in the i^{th} row of matrix ***B*** there will be more than one place, where unit value will exist. This is clearly represented by Boolean matrix for flow sequence, b, given below; in which feed stream is splitted to enter in effect nos. 6 and 7, thus unit value exists at two places in the first column and 6^{th} & 7^{th} rows. Further, these splitted streams enter into 5^{th} effect giving rise to two entries of unit value in

5th row and 7th and 8th columns, which represent effect nos. 6 and 7, respectively. Similarly, Boolean matrices for condensate and liquor flashing are drawn.

$$\boldsymbol{B} = \begin{bmatrix} 0 & 0 & 1 & 0 & 0 & 0 & 0 & 0 \\ 0 & 0 & 0 & 1 & 0 & 0 & 0 & 0 \\ 0 & 0 & 0 & 0 & 1 & 0 & 0 & 0 \\ 0 & 0 & 0 & 0 & 0 & 1 & 0 & 0 \\ 0 & 0 & 0 & 0 & 0 & 0 & 1 & 1 \\ 1 & 0 & 0 & 0 & 0 & 0 & 0 & 0 \\ 1 & 0 & 0 & 0 & 0 & 0 & 0 & 0 \\ 0 & 1 & 0 & 0 & 0 & 0 & 0 & 0 \end{bmatrix}$$

It should be noted that in the present investigation to select the optimal F, one has to re-configure the Boolean matrix only which is an input data file to the computer program and need not derive the model equations for each F separately.

5. Validation of model

To establish the reliability of the present model it is required to compare the results predicted from simulation with the plant data obtained from a nearby paper mill.

Fig. 9 and 10 have been plotted to show the comparison between data of the mill for concentration of black liquor and vapor body temperature of different effects with that obtained from model respectively. Predicted results show that the liquor concentration match within an error band of -0.2 to +0.4%, and the vapor temperature of different effects match within a error limit of –0.26 to +1.76%. The present model computes the temperature difference (ΔT) for each effect with a maximum relative error of 23% between plant data and simulation result. However, for the similar MEE system the published model (Bremford and Muller-Steinhagen, 1994) reported a maximum error of 43.43% for the prediction of temperature difference in each effect. Thus, it appears that the present model predicts the plant data fairly well in comparison to the published model.

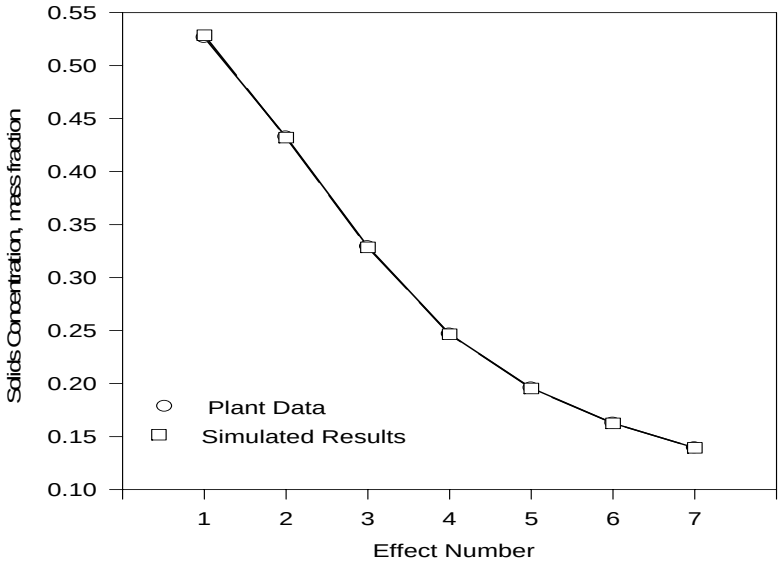

Fig. 9 Comparison between Solid concentration in liquor from plant data and that predicted by model

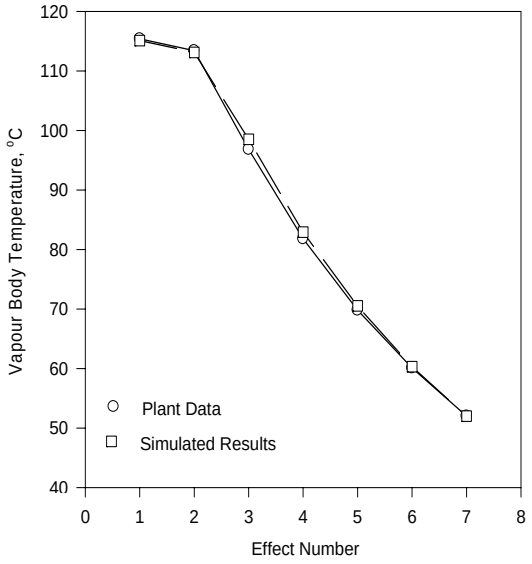

Fig. 10 Comparison between vapor temperature of different effects from Plant Data and that from model

6. Selection of optimal F

A SEFFFE system employed in a Paper Mill can be operated under different operating strategies, which include different flow sequences as detailed in Table 4. The SEFFFE system considered in the present work includes feed-, product- and condensate- flashing as well as

feed and steam splitting. Out of the above referred operating strategies, selection of proper F, which will provide maximum SE, is the aim of the present study. In fact, in real situation, the best F is not only decided by SE but also based on other parameters such as foaming of feed, scaling of tubes, etc. Nevertheless, grading of F based on SE has always been an important step towards finalization of best flow sequence which depends on SE data and operating convenience.

To screen the optimal F amongst the feasible F, it is necessary to study the effect of variation of input parameters T_0 and F on output parameter, SC and SE. It will help to select an optimal F, which will remain as optimal for complete range of operating parameters given in Table 2. It is well known fact that a change in input parameters triggers a complex chain reaction affecting almost all output parameters, including, vapor body and liquor temperatures from first to sixth effect, almost all flash vapor fractions, heat transfer coefficients, rate of evaporation in each effect, Q_{loss} from each effect and amount of heat rejected to atmosphere with condensate. It appears that SE is the single most prominent parameter to evaluate the efficiency of the system as it varies with variation in operating parameters and geometrical parameters as well. SE also directly affects the economy of the operation. Nevertheless, the study of variables towards the variation of SC with input parameter offers better understanding.

6.1. Effect of variations of T_0 and F on SC and SE for all F

An investigation based on the present model has been undertaken to study the effect of steam temperature, T_0, and feed flow rate, F, on SC and SE, which is carried out for different flow sequences a, b, c, d, e and f as defined in Table 4.

6.1.1. Effect of steam temperature

Fig. 11 shows the effect of steam temperature, T_0, on SC for F, a, b, c, d, e and f and shows that the value of SC increases with the increase in steam temperature for all the flow

sequences investigated. However, for a given value of steam temperature, SC for different F are markedly different. In fact, SC for backward flow sequence is minimum whereas, SC for the flow sequence 'f' is maximum followed by e, d, c, b and a in decreasing order.

The effect of T_0 on SC is attributed to the decrease in latent heat of condensation of the steam with the increase in the saturation temperature. Further, an increase in the steam temperature, increases the temperature difference between steam and liquor, thus provides conducive environment to pump more heat in to the effect causing more evaporation. The combined effect, of above factors, is such that the value of SC increases with increase in T_0.

In the present system live steam is used in first two effects of the SEFFFE system. When any operating strategy like F is changed it alters the SC of these two effects.

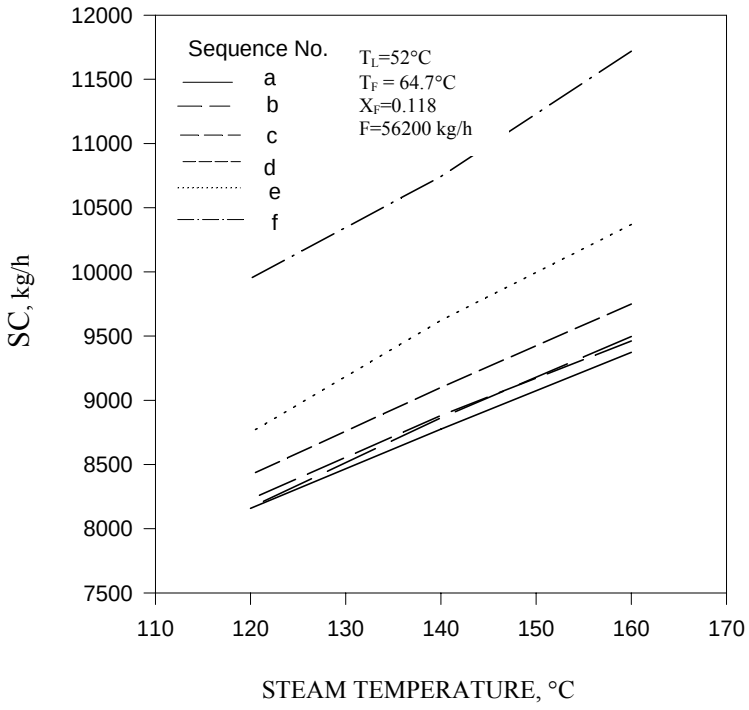

Fig. 11. Effect of T_0 on SC for feed sequence a to f

The variation in the values of SC for F, a to f, for a given value of T_0 can be explained as follows: The SC for a flow sequence mainly depends on values of two factors: U and driving

force (ΔT) available for transfer of heat across the steam chest of an effect as the heat transfer area of all the effects are constant. As live steam is fed to effect no. 1 and 2, the product of above two factors (U ΔT) are computed for these effects for all flow sequences and are shown in Fig. 12. From this figure, it can be noted that values of (U ΔT) in first two effects are decreasing in the following order of flow sequences: f, e, d, c, b and a. As areas of first two effects are constant similar order as observed in case of U ΔT is also observed for SC.

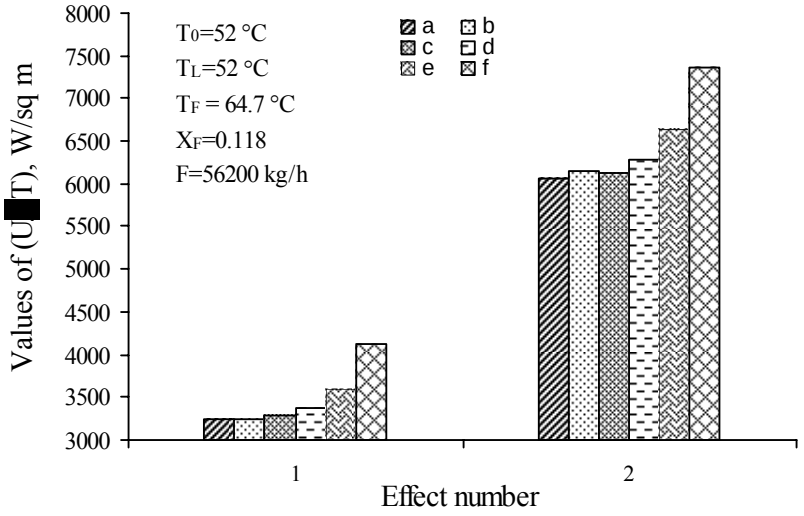

Fig. 12. Values of (UΔT) in first two effect for six FFSs

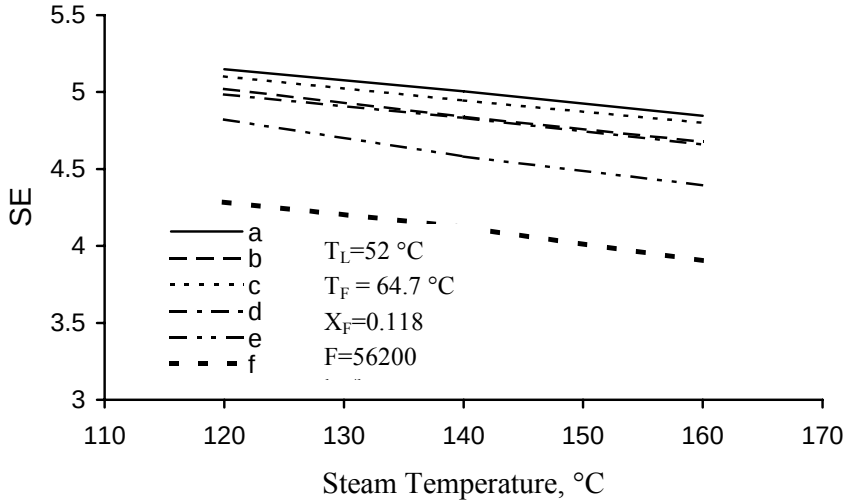

Fig. 13. Effect of T_0 on SE for feed sequence a to f

Fig. 13 shows the effect of T_0 on value of SE for different flow sequences a, b, c, d, e and f. The figure clearly indicates that SE gradually decreases with the rise in steam temperature. The maximum SE is observed for F ‘a’ followed by c, b, d, e and f in decreasing order. However, the values of SC for F, b and d, are close to each other.

For a given F the value of SE mainly depends on total water to be evaporated and live steam consumed to carry out the above evaporation. To show the variation of SC, SE and total evaporation with change in F, Fig. 14 is drawn in which fractional values of these parameters for F, b to f, with respect to ‘a’ are plotted for base case operating conditions, given in Table 1. The fractional value of SC for flow sequence, b with respect to a is defined as,

$$= \frac{Amount\ of\ SC\ for\ flow\ sequence, b}{Amount\ of\ SC\ for\ flow\ sequence, a}$$

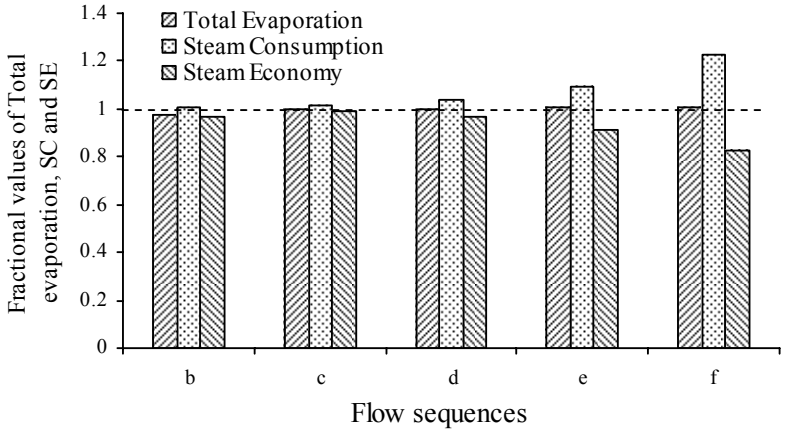

Fig. 14. Total evaporation, SC and SE for flow sequences 'b' to 'f' with respect to 'a'

Similarly, fractional values of other parameters are obtained and shown in Fig. 14. The dotted line in this figure shows the fractional values of SC, SE and total evaporation for F ‘a’ which is obviously unity. This line is used for the sake of comparison of other F with that of ‘a’.

Fig. 14 shows that the total water evaporated for flow sequences, d, e and f is slightly more (within +1%) than that for ‘a’. For F ‘c’ fractional value of total water evaporated is nearly unity whereas for F ‘b’ it is less by 2.32 % in comparison to ‘a’. As a result, the product

concentration, x_P, is different for different F. However, the fractional values of SC for F, 'b' to 'f' are greater than unity and continuously increase from F, 'b' to 'f'. It is clear from Fig. 14 that the increase in the value of SC is much more than increase in total evaporation for F, d, e and f in comparison to 'a'. Hence, the values of SE for these F are considerably less. It is also noted from Fig. 14, that total evaporation for flow sequence, 'c' is equal to that of 'a', whereas, SC for 'c' is greater by 1.2% in comparison to 'a'. The cumulative effects of these factors lower the value of SE for flow sequence 'c'. It is further observed from Fig. 14, that for F 'b' total evaporation is less and SC is slightly more than that for 'a'. As a result of it the value of SE is lowest for F 'b'.

6.1.2. Effect of feed flow rate

Table 9 shows the effect of variation of feed flow rate on UΔT, total evaporation, SC and SE for different flow sequences a, b, c, d, e and f.

Table 9 shows that the value of SC increases with the increase in black liquor feed rate. For lowest value of feed flow rate, the SC is highest for F, f followed by e, d, c, b and a in decreasing order. However, at highest flow rate the F f, e, d, c, a and b are in order of decreasing value of SC.

Further, Table 9 indicates that for a flow sequence the value of SE decreases with increase in feed flow rate and the maximum SE is observed for the F 'a' followed by c, b, d, e and f.

When feed flow rate is increased the U of different effects increase. This in turn increases heat flow to each effect and causes the temperature of each effect to increase due to formation of higher amount of vapor in each effect, which subsequently pressurizes the vapor body to some extent. This rise in temperature will have a reverse effect on heat transfer rate as it decreases the driving force ΔT. However, the overall effect will be governed by the product UΔT. As the behaviors of first two effects affect the SC most, UΔT values of only these effects are reported in Table 9. From the simulated results, shown in Table 9, it is evident that

UΔT increases with increase in feed flow rate and thus the value of SC also increases with feed flow rate.

Table 9

Values of UΔT, total evaporation, SC and SE for minimum and maximum feed flow rate

Parameter(s)		a	b	c	d	e	f
Feed flow rate = 56200 kg/h							
UΔT, W/m^2	1	3236.3	3240.4	3285.8	3380.1	3600.8	4131.3
	2	6062.5	6140.6	6128.4	6276.9	6635.6	7357.1
Total evaporation, kg/h		43916.6	42897.3	43916.4	43961	44076.4	44270.9
SC, kg/h		8776	8863	8881.2	9100	9622	10742.6
SE		5.00	4.84	4.94	4.83	4.58	4.12
Feed flow rate = 78680 kg/h							
UΔT, W/m^2	1	4035.6	3919.4	4116.7	4317.7	4757.1	6133.4
	2	7852.6	7928.1	7921	8139.6	8597.2	9924.8
Total evaporation, kg/h		49450.3	47876.8	49468.6	49592.4	50278.2	51521.7
SC, kg/h		11184	11154.5	11322.3	11702.2	12512.7	14954.3
SE		4.42	4.29	4.37	4.24	4.02	3.45

Table 10 shows the percent variation in the values of UΔT, total evaporation, SC and SE with change in feed flow rate from 56200 to 78680 kg/h (a 40 % increase) for different flow sequences. This table presents the data of Table 9 in a different manner. Table 10 clearly shows that the values of UΔT in first two effects increase with increase in feed flow rate resulting in higher SC in all F. However, the average value of UΔT of first two effects increases by 27 % when the feed rate is changed from 56200 to 78680 kg/h for F ‘a’ and the value of UΔT increases by 41.7 % for F ‘f’ for the same variation in feed rate. Due to this, the

percent increase in SC for different F with feed flow rate is in the following order: b > (a = c) > (d = e) > f.

As can be seen from Table 10, total evaporation as well as SC increase for all the flow sequences with the increase in feed flow rate. However, the cumulative effect is such that the SE decreases with the increase in feed flow rate. For example, for 'a' when feed rate is increased from 56200 to 78680 kg/h the amount of total water evaporated increases by 12.6% where as SC rises by 27.44 %. The cumulative effects of above parameters decrease the SE by 11.64%. Similar behavior is seen for other F also. Further, it is observed that the flow sequences 'a', 'b' and 'c' almost behave similarly as far as SE is concerned.

Table 10

Percent Variations in UΔT, total evaporation, SC and SE when the feed flow rate in increased by 40%

Parameter(s)		a	b	c	d	e	f
UΔT, W/m^2	1	24.70	20.95	25.29	27.74	32.11	48.46
	2	29.53	29.11	29.25	29.67	29.56	34.90
Total evaporation, kg/h		12.60	11.61	12.64	12.81	14.07	16.38
SC, kg/h		27.44	25.85	27.49	28.60	30.04	39.21
SE		-11.64	-11.32	-11.64	-12.28	-12.28	-16.40

From the above investigations, it is clear that for the present SEFFFE system, backward F is found to be the optimal F as it offers highest value of SE for complete operating range of parameters. It is interesting to note that the present SEFFFE system employed in a nearby Indian Kraft paper industry also operates under backward F to achieve maximum SE.

7. Conclusions

The salient conclusions drawn from the present investigations are:

1. The empirical correlation of U for a SEFFFE system predicts the plant data within ±10%.
2. The present model computes the liquor concentration profile and vapor body temperature profile of different effects within maximum error limit of ±2%.
3. The model developed in the present paper can work as an effective screening tool for the selection of optimal $\underline{F}$.
4. Out of the different $\underline{F}$ investigated for SEFFFE system, the backward $\underline{F}$ was found to be optimal leading to highest value of SE.

Nomenclature

A	Heat transfer area of an effect, m^2
a	Coefficients of Eq. 14
a_1 - a_4	Coefficients of cubic polynomial (Eq. 9)
a_{ij}	Element of the inverse matrix of [**Y – I**]
b	Coefficients of Eq. 14
b_{ij}	A parameter used in Table 8
τ	Boiling Point Rise, K
c	Coefficients of Eq. 14
C_1 - C_5	Constant in mathematical model
CO	Condensate flow rate, kg/s
C_{PP}	Specific heat capacity of black liquor, J/kg/K
d	Coefficients of Eq. 14
F	Feed flow rate, kg/s
$\underline{F}$	Feed flow sequence
h	Specific enthalpy of liquid phase, J/kg
H	Specific enthalpy of vapor phase, J/kg

I	Identity matrix
k	Iteration number
L	Liquor flow rate, kg/s
MEE	Multiple effect evaporator
n	Number of total effects
n_s	Number of effects supplied with live steam
P	Pressure of steam and vapor bodies of evaporator, N/m^2
PI	Performance Index as defined in Eq. 23
Q_{loss}	Heat loss from an evaporator, W
SC	Steam consumption, kg/h
SE	Steam economy
SEFFFE	Septuple effect flat falling film evaporator
T	Vapor body temperature of an effect, K
U	Overall Heat Transfer Coefficient, $W/m^2/K$
V	Rate of vapor produced in an evaporator, kg/s
x	mass fraction of solids in liquor
Y	Flow fraction matrix

Subscripts

avg	Average of inlet and outlet conditions
e	Exit condition
F	Feed
i	Effect number
L	Black Liquor
0	Steam
V	Vapor

Greek Characters

α	A parameter as defined by Eq. 25
β	A parameter as defined in Eq. 34
Δ	Difference between two parameter
δ	Difference between same variable over two successive iterations
Υ	A parameter as defined in Eq. 40
Υ'	A parameter as defined in Eq. 39
Υ''	A parameter as defined in Eq. 41
θ	A parameter as defined in Eq. 29

References

1. Ayangbile, W.O., Okeke, E.O., & Beveridge, G.S.G. (1984). Generalised Steady State Cascade Simulation Algorithm in Multiple Effect Evaporation. *Comp. Chem. Eng., 8*, 235-242.
2. Bhargava, R. (2004). *Simulation of flat falling film evaporator network*. Ph.D. Dissertation, Department of Chemical Engineering, Indian Institute of Technology Roorkee, India.
3. Bremford, D.J., & Muller-Steinhagen, H. (1994). Multiple effect evaporator performance for black liquor-I Simulation of steady state operation for different evaporator arrangements, *Appita J.*, *47*, 320-326.
4. Coulson, J.M. and Richardson, J.F. (1996). Chemical Engineering, Vol. 1, 5th Edn, Butterworth Heinemann Ltd.
5. El-Dessouky, H.T., Alatiqi, I., Bingulac, S., & Ettouney, H. (1998). Steady state analysis of the multiple effect evaporation desalination process, *Chem. Eng. Tech.*, *21*, 15-29.

6. El-Dessouky, H.T., Ettouney, H.M., & Al-Juwayhel, F. (2000). Multiple effect evaporation-vapor compression desalination processes, *Trans IChemE*, *78*, Part A, 662-676.

7. Harper, J.M., & Tsao, T.F. (1972). Evaporator strategy and optimization. *In Computer Programs for Chemical Engineering Education*, VI Design, Ed. R. Jelinek, Aztec Publishing, Austin, Texas.

8. Holland, C.D. (1975). Fundamentals and Modelling of Separation Processes. Prentice Hall Inc., Englewood cliffs, New Jersey.

9. Itahara, S., & Stiel, L.I. (1966). Optimal Design of Multiple Effect Evaporators by Dynamic Programming, *Ind. Eng. Chem. Proc. Des. Dev.*, *5*, 309.

10. Kern, D.Q. (1950). Process Heat Transfer, McGraw Hill.

11. Lambert, R.N., Joye, D.D., & Koko, F.W. (1987). Design calculations for multiple effect evaporators-I linear methods, *Ind. Eng. Chem. Res.*, *26*, 100-104.

12. Mathur, T.N.S. (1992). *Energy Conservation Studies for the Multiple Effect Evaporator House of Pulp and Paper Mills*. Ph.D. Dissertation, Department of Chemical Engineering, University of Roorkee, India.

13. Nishitani, H., & Kunugita, E. (1979). The optimal flow pattern of multiple effect evaporator systems. *Comp. Chem. Eng., 3*, 261-268.

14. Radovic, L.R., Tasic, A.Z., Grozanic, D.K., Djordjevic, B.D., & Valent, V.J. (1979). Computer design and analysis of operation of a multiple effect evaporator system in the sugar industry, *Ind. Eng. Chem. Proc. Des. Dev*, *18*, 318-323.

15. Rao, N. J., & Kumar, R. (1985). Energy Conservation Approaches in a Paper Mill with Special Reference to the Evaporator Plant. *Proc. IPPTA Int. Seminar on Energy Conservation in Pulp and Paper Industry*, New Delhi, India, 58-70.

16. Ray, A.K., Rao, N.J., Bansal, M.C., & Mohanty, B. (1992). Design Data and Correlations of Waste Liquor/Black Liquor from Pulp Mills", *IPPTA J.*, *4*, 1-21.

17. Ray, A.K., & Singh, P. (2000). Simulation of Multiple Effect Evaporator for Black Liquor Concentration, *IPPTA J.*, *12*, 53-63.

18. Stewart, G., & Beveridge, G. S. G. (1977). Steady State Cascade Simulation in Multiple Effect Evaporation. *Comp. Chem. Eng., 1*, 3-9.

19. Süren, A. (1995). *Scaling of black liquor in a falling film evaporator*, Master Thesis, Georgia Institute of Technology, Atlanta, GA.